FOREX Publication
Open Access | Rapid and quality publishing

International Journal of Electrical and Electronics Research (IJEER)
Research Article | Volume 13, Issue 1 | Pages 132-137 | e-ISSN: 2347-470X

Ultra-High Photosensitivity of Nb_2O_5/Ge Prepared *via* Direct Current Reactive Magnetron Sputtering Technique

Abdullah Ahmed[1], Dr. Ehsan Sabbar[2], and Dr. Ahmed Abbas[3]*
[1,2,3]*College of Engineering, University of Anbar, Iraq;* [1]*abdullahkhalid.ahmed@uoanbar.edu.iq;*
[2]*ehsan.sabbar@uoanbar.edu.iq;* [3]*ahmed.abbas@uoanbar.edu.iq*

***Correspondence:** *abdullahkhalid.ahmed@uoanbar.edu.iq*

ABSTRACT- The primary objective of this research is to fabricate and evaluate Nb_2O_5 thin films prepared *via* DC (direct current) reactive magnetron sputtering at target powers of 25 W, 50 W, and 75 W, deposited on quartz substrates and Ge wafers. The structural and morphological characteristics of the fabricated Nb_2O_5 thin films were analyzed using XRD (X-ray diffraction) and FE-SEM (field emission scanning electron microscopy), while their electrical and optical properties were characterized using UV-Vis spectrophotometry and I-V (current-voltage) tests. XRD results confirmed a natural polycrystalline structure with a hexagonal lattice, while FE-SEM imaging revealed uniform deposition and strong dependence of nanostructure size and configuration on deposition parameters. EDS (Energy-Dispersive Spectroscopy) analysis showed an increase in Nb content with higher sputtering power. The thin films demonstrated significant photosensitivity at a wavelength of 350 nm, achieving a maximum response of 514.89% at a sputtering power of 50 W. Although 350 nm was the primary wavelength tested, the UV-Vis absorbance spectra revealed a broader detection range in the UV spectrum, influenced by the DC sputtering power. Higher sputtering powers enhanced absorption in the UV range, attributed to improved film crystallinity and reduced defects, which sharpened the absorption edge. Further studies are required to assess the UV photosensitivity at additional wavelengths and determine the detection range comprehensively. Additionally, the dynamic potential of the sensors was evaluated through time-dependent response tests, indicating rapid rise and fall times suitable for real-time UV detection. These findings suggest that Nb_2O_5 thin films are promising candidates for visible-blind UV detectors and optoelectronic circuits, particularly in the UV-A range.

Keywords: Nb_2O_5, Photosensitivity, Magnetron Sputtering, Thin Films, Photodetectors.

ARTICLE INFORMATION

Author(s): Abdullah Ahmed, Dr. Ehsan Sabbar, and Dr. Ahmed Abbas;

Received: 04/10/2024; **Accepted**: 05/01/2025; **Published**: 30/03/2025;
e-ISSN: 2347-470X;
Paper Id: IJEER 0410-03;
Citation: 10.37391/IJEER.130117
Webpage-link:
https://ijeer.forexjournal.co.in/archive/volume-13/ijeer-130117.html

Publisher's Note: FOREX Publication stays neutral with regard to Jurisdictional claims in Published maps and institutional affiliations.

1. INTRODUCTION

Recently, thin films of oxide semiconductors have garnered significant attention from the technological community due to their diverse applications in electrochromic and photovoltaic systems, catalysis, batteries, and electronic devices such as memristors [1,2]. Among these materials, niobium oxide (Nb_2O_5) stands out as a particularly promising candidate due to its unique combination of electrical and optical properties. Nb_2O_5 thin films exhibit a high UV-Vis-NIR (Ultraviolet-Visible-Near Infrared) transparency, a high refractive index, and exceptional permittivity, making them suitable for numerous advanced technological applications [3].

Nb_2O_5 thin films are versatile and widely used in microelectronics, serving as electronic gate materials, optical components, gas sensors, UV filters, photoelectrodes, high-density energy capacitors, optical protective coatings, and electrochromic devices [4]. With the Sun emitting UV radiation in the 200–400 nm range, the UV-A band (320–400 nm) is particularly significant as it reaches the Earth's surface. Prolonged exposure to UV-A radiation is associated with an increased risk of skin cancer, necessitating effective monitoring and detection of UV-A radiation [5–9].

Nb_2O_5 thin films have been deposited using various techniques—including spray pyrolysis, sol-gel methods, photochemical vapor deposition, thermal oxidation, IBS (ion beam sputtering), electron beam evaporation, DC/RF plasma magnetron sputtering, and PLD (pulsed laser deposition) [10]. The sputtering method stands out for its rapid deposition process. This method enables the production of thin films with excellent cleanliness, adherence, homogeneity, and repeatability. Additionally, commercially available sputtering techniques provide high conductivity and transparency, ensuring uniform layer thickness across large substrate areas [11–14].

The novelty of the presented work lies in the fabrication of Nb_2O_5 thin films using DC reactive magnetron sputtering to achieve superior photosensitivity and rapid UV-A detection compared to similar oxide films, such as Ni (nickel) oxide, reported in the literature. This study distinguishes itself by systematically examining the influence of sputtering power on the structural, morphological, optical, and sensing properties of the films. Furthermore, the integration of Nb_2O_5 films with Ge wafers enhances their dynamic photosensitivity, making them ideal for visible-blind UV detection in the UV-A range.

FOREX Publication
Open Access | Rapid and quality publishing
International Journal of Electrical and Electronics Research (IJEER)
Research Article | Volume 13, Issue 1 | Pages 132-137 | e-ISSN: 2347-470X

The specific goals of this research are to:
1. Investigate the structural and morphological properties of Nb_2O_5 thin films prepared at varying DC sputtering powers using XRD and FE-SEM.
2. Characterize the optical properties, focusing on sensitivity to UV-A radiation, detection range, and energy band gap determination.
3. Evaluate the electrical and dynamic sensing capabilities, including sensitivity, photosensitivity, and time-domain response under UV illumination.

By addressing these parameters, this study aims to contribute significantly to the development of high-performance Nb_2O_5-based UV-A photodetectors and optoelectronic devices.

2. EXPERIMENTAL METHOD

This research seeks to study the effect of varying sputtering power during the deposition process on such properties as microstructure, optical properties, and electrical properties of Nb_2O_5 thin films. For assessing the characterization of the structure, morphology, and optical performance, the films were prepared on quartz substrates with an area of (1.5×1.5) cm^2. Further electrical measurements were also conducted on the wafers of *Ge*. The deposition was performed at various sputtering powers with the value of 25, 50 and 75 watts by using the DC reactive magnetron technique. The target was a niobium disk with a diameter of 5 cm, a thickness of 3mm, a purity of 99.99%, a density of 8.57 g/cm^3, and a melting point of 2,468°C. To measure the discharge current, it was placed 5 cm away from the anode.

An ultrasonic bath with deionized water and isopropanol was used to clean the quartz substrates before the deposition process, followed by drying with nitrogen gas. Oxygen served as the reactive gas, while argon, with a purity of 99.99%, was used as the sputtering gas. Before initiating the sputtering procedure, a diffusion pump evacuated the chamber until the 4.2 x 10-3 Pa of base pressure was reached, maintaining an operational pressure of 4.0 Pa. A mass flow controller was used to introduce *Ar* sputtering gas and oxygen-reactive gas into the vacuum chamber during the sputtering process, with the reactive *Ar* gas flowing at a steady rate of 50 standard cubic centimeters per minute (sccm), and O_2 at 5 sccm. The deposition time was 120 minutes.

Thin films underwent annealing in air for one hour at 800 °C temperature after deposition. The study utilized a Shimadzu XRD-6000 X-ray diffraction apparatus with CuKα radiation (wavelength = 0.154 nm) within the 2θ range of 10° to 90°. An energy-dispersive system integrated into the MIRA3 TESCAN model was used for imaging and analysis via SEM, operating at an applied voltage of 10 kV. Shimadzu UV-1650 PC (UV-VIS spectrophotometer) measured the spectrum of optical absorption and the optical energy gap of the thin films that were deposited with wavelengths between 330 and 100 nm. Film thicknesses (280, 520, and 848 nm) were precisely determined through cross-section imaging with FESEM.

Light sensitivity testing was carried out using a Fluke model 8846A digital electrometer, and photo response measurements of photodetectors under dark and illumination were taken under zero bias voltage. The spectral responsivity of the UV-A photodetector was obtained using an RF-551 Spectrofluorimetric detector, featuring a 200 W Hg (Xe) lamp as a light source, and a monochromator linked to a PC with Visual Basic 5 software, as shown in *figure 1*.

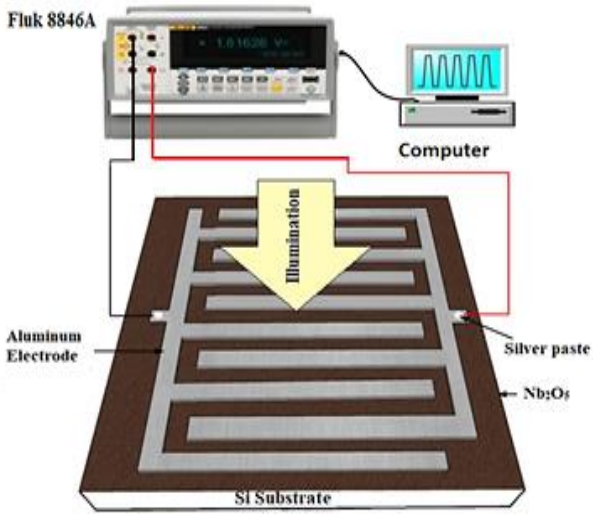

Figure 1. Setup for measuring photoconductivity

3. RESULTS AND DISCUSSION

3.1. X-Ray Diffraction Analysis

An XRD study was conducted to evaluate the crystallinity and structure of the Nb_2O_5 films that were formed at power levels (25 W - 75 W) with a 25 W increment. The findings of this analysis are shown in figure 2. All of the films exhibited polycrystalline crystal structures based on the XRD findings. It displayed peaks at 2θ = 22.43°, 28.81°, 36.80°, and 46.09°, which, in turn, correspond to the hexagonal phase (001), (100), (101), and (002) planes of Nb_2O_5. This outcome is consistent with a prior study [9]. With the number 00-028-0317, every single one of these spikes can potentially be indexed to the JCPDS card. Additionally, all films exhibited a preferential orientation in the (001) direction at a diffraction angle of 2θ = 22.43°. The preferred orientation gradually intensified when the DC power of sputtering increased from 25 to 75 W, especially for the planes (001) and (100), demonstrating an improvement in the crystallinity of the Nb_2O_5 films. Three diffraction lines generated for the (110), (102), and (004) lattice planes with diffraction angles of 50.67°, 55.18°, and 58.97°, respectively, as the DC power was increased. This resulted in a rise in the sample's crystallinity. In addition, the Scherrer formula utilizing the (001) diffraction line revealed that the highest peak levels in the diffraction lines becoming broader corresponded to an increase in the size of the crystallites. When the DC power was increased from 25 to 75 W, the crystallites' size grew from 21.3 to 24.9 nm.

FOREX Publication
Open Access | Rapid and quality publishing
International Journal of Electrical and Electronics Research (IJEER)
Research Article | Volume 13, Issue 1 | Pages 132-137 | e-ISSN: 2347-470X

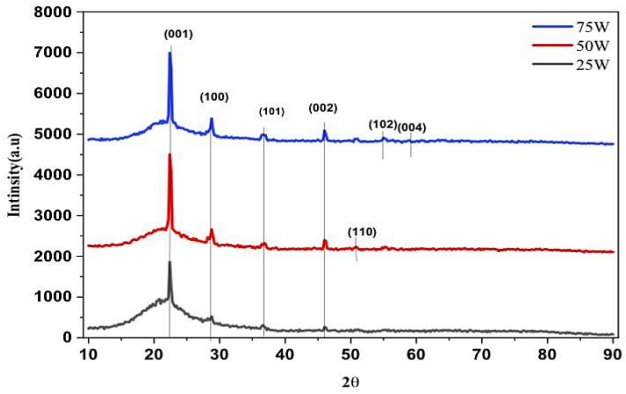

Figure 2. XRD patterns Nb_2O_5 thin film made at the room temperature utilizing various DC powers

3.2 Optical Properties

From the UV-VIS optical absorbance figure, we identified a peak indicative of a highly absorbent region. By noting the absorbance value (*A*) at this peak and referencing the associated sample thickness (*t*), and using *equation (1)* to measure the value of the absorption coefficient α [7].

$$\alpha = 2.303\frac{A}{t} \qquad (1)$$

Both crystalline and amorphous materials display a notable characteristic in their fundamental absorption edges. To determine the band gap of the material, comprehending how the valence band moves into the conduction band is vital. The energy band gap (E_g) was determined using the calculation presented in *equation (2)*[8].

$$\alpha hv = B\left(hv - E_g\right)^r \qquad (2)$$

Where the optical energy gap is represented by E_g, the structure-dependent constant *B* is represented by a constant, and *r* is the optical absorption index. Depending on the electronic transition type that causes the absorption, *r* may have a value of 1/2, 3/2, 2, or 3[8]. The absorption coefficient values of electromagnetic radiation at each wavelength in the spectrum were calculated using UV-Vis spectra. There are direct optical transitions since the experimental results match the value of r-coefficient (0.5) better in comparison to the other factors [9]. Figure 3(a) illustrates the Nb_2O_5 thin films optical absorbance curves for the produced using variable DC powers between 200 and 800 nm in wavelength at room temperature. The films present an increased absorption in the ultraviolet (UV) spectrum and low absorption in the wavelength range that is visible. As the DC power increases, absorbance also rises, attributed to the heightened sputtering power, resulting in an increase of the thin film thickness. Additionally, as the DC power increases, the absorption edge transitions from gradual to sharper. It is explained by a decrease in lattice imperfections and the elimination of tail states close to the band edges [10].

The presented $(\alpha hv)^2$ against the *hv* (photon energy) plot for the Nb_2O_5 thin films using various DC powers at room temperature is depicted in *figure 3(b)*, as stated by previous studies of direct transition of Nb_2O_5 [11]. From the tangent line intersection with the x-axis, the band gap was calculated. It has been noted that when DC power increases, the direct optical energy gap decreases. As the X-ray diffraction shows, this decreased results from increasing the crystallite size because of a decrease in the effect of quantum confinement and a high influence at the nano-size. There has been evidence in earlier research that a rise in DC power causes the optical energy gap to reduce; The band gaps discovered in this study are in agreement with those findings in [12]. The photogenerated carriers at 350 nm are arise from the photo responsive flaws found in the band gap. This conclusion is in line with earlier research on zinc oxides [11] and tin sulphide [14], which also mentioned that under lower energy band gap illumination, intrinsic flaws in zinc oxide and tin sulfide that caused detection were observed.

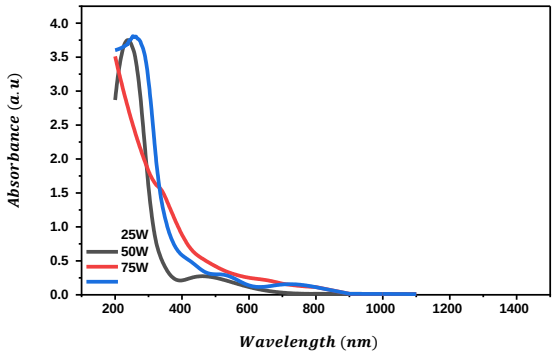

(a)

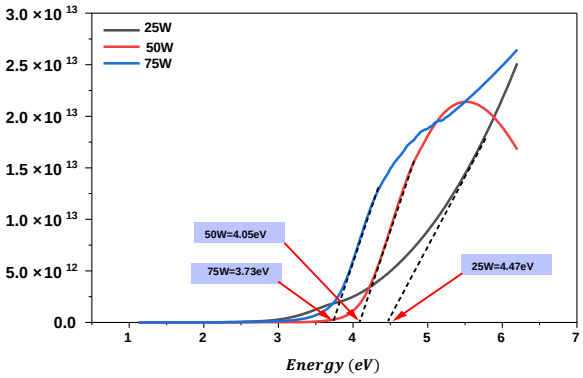

(b)

Figure 3. (a) UV-VIS optical absorbance for the ZnO/Nb_2O_5 thin films produced at room temperature using various DC powers; (b) (αhv)2 versus (hv) for ZnO/Nb_2O_5 thin films produced with various DC powers at the RT

3.3 Characteristics of I-V

The analysis of the photoconductive detector's I-V curve was conducted under both dark and illuminated conditions to evaluate the electrical performance of the Nb_2O_5 thin films fabricated at 25 W, 50 W, and 75 W sputtering powers. *Figure 4* presents the typical current-voltage characteristics of the films under specific illumination conditions. The light conditions were defined with a 350 nm UV wavelength and intensities ranging from 50 mW/cm² to 150 mW/cm². Sweep voltages between -1 V and +1 V were applied during the measurements.

FOREX Publication
Open Access | Rapid and quality publishing
International Journal of Electrical and Electronics Research (IJEER)
Research Article | Volume 13, Issue 1 | Pages 132-137 | e-ISSN: 2347-470X

Under illumination, an increase in light intensity resulted in a corresponding rise in photocurrent, attributed to the generation of additional electron-hole pairs. The behavior of the films in the low voltage range (0 to 0.35 V) was dominated by recombination current. In this region, intrinsic carrier concentrations were lower than the combined minority and majority carrier concentrations (where $n_i^2 < n_p^2$), leading to minor increases in current. This is explained by the stimulation of electrons transitioning from the valence band (V.B.) to the conduction band (C.B.), where recombination with existing holes in the V.B. occurs. Consequently, the recombination current exhibited only slight increases in this low-voltage region.

At higher voltages, diffusion current became predominant, characterized by an exponential and rapid increase in current with applied voltage. This phenomenon is associated with the efficient transport of charge carriers across the junction. However, differences in reverse bias current were observed among the samples fabricated at varying sputtering powers.
For the 25 W sample, the reverse bias current was higher compared to the samples fabricated at 50 W and 75 W. This behavior can be attributed to the presence of a greater number of defects and dislocations in the 25 W film, which impair charge carrier mobility and serves as recombination sites, thereby increasing leakage current. Conversely, the films deposited at higher powers (50 W and 75 W) demonstrated improved crystallinity and reduced defect density, resulting in a lower reverse bias current. This trend indicates that higher sputtering powers enhance film quality, reducing recombination losses and improving charge carrier transport properties.

Figure 4 illustrates the I-V characteristics of the Nb_2O_5 thin films under dark and illuminated conditions. The illumination conditions and corresponding light curves are shown for each sample, highlighting the increase in photocurrent with rising light intensity. The films fabricated at 50 W demonstrated the most balanced performance, achieving lower reverse current and higher photocurrent under illumination, making them optimal for photodetector applications.

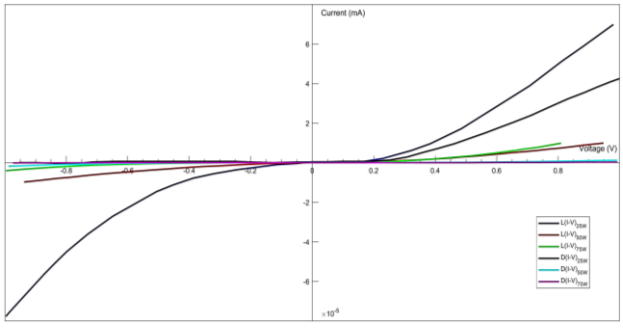

Figure 4. I-V characteristics of Nb_2O_5 thin films formed at various powers (25 W, 50 W, and 75 W) when lighted and in the dark, respectively

Dynamic resistance is considered the inverse of the slope of the I-V curve at a specific operating point, reflects the material's response to changes in voltage and current. It is calculated from the I-V characteristics of Nb_2O_5 thin films. *table 1* demonstrates the dynamic resistances of Nb_2O_5 thin films formed at various powers (25 W, 50 W, and 75 W) when lighted and in the dark.

Table 1. Dynamic resistance (Rd) for Nb_2O_5 thin films at different DC powers

Voltage (V)	Dynamic resistance (R_d) at 25 W		Dynamic resistance (R_d) at 50 W		Dynamic resistance (R_d) at 75 W	
	Illuminated (Ohms)	Dark (Ohms)	Illuminated (Ohms)	Dark (Ohms)	Illuminated (Ohms)	Dark (Ohms)
-0.8	2.50	200.00	1.60	333.33	1.11	666.67
-0.6	1.67	133.33	1.25	250.00	0.89	333.33
-0.4	1.00	100.00	1.00	200.00	0.67	200.00
-0.2	0.67	66.67	0.80	160.00	0.50	133.33
0.0	0.50	50.00	0.67	133.33	0.40	100.00
0.2	0.40	40.00	0.50	100.00	0.33	80.00
0.4	0.36	33.33	0.40	80.00	0.29	66.67
0.6	0.33	30.00	0.36	66.67	0.25	55.56
0.8	0.31	26.67	0.33	55.56	0.22	50.00
1.0	0.29	22.22	0.29	50.00	0.20	44.44

The average power output of a photovoltaic system categorized by different times of the day and various irradiance levels: Morning 144.91W, Midday 139.89W, Afternoon 100.00 W, Evening 100.00W, Average Power Out- put by Irradiance Level (B).

3.4 Photosensitivity

One of the important factors influencing the photodetector quality is sensitivity (S), which is determined by equation (3)[14].

$$S(\%) = \frac{\Delta I_\lambda}{I_{dark}} \times 100\% \qquad (3)$$

where $\Delta I_\lambda = I_{light} - I_{dark}$ is the photocurrent, I_{light} is the light current, and I_{dark} is the dark current. In simpler terms, sensitivity is the amount of current that increases in a thin film in response to light illumination.

This phenomenon occurs when a photodetector is exposed to light at a specific wavelength. For a predetermined period of time, the UV-A photodetector will react by turning on and off. The photodetector's rising time (t_r) and fall time (t_f) in accordance to the pulse signal with square waves are described in the time domain. The time interval that needs to elapse before the detector's output can climb from 10% to 90% of its peak value under rapid illumination is known as the rise time (t_r). As illustrated in *figure 5*, selecting a quantity equal to one-tenth of the shortest length of a pulse discovered by the rising time of the detector is a good general rule of thumb for handling any situation. The detector takes some time to brighten back up to its typical level after the light is turned off. This is the period of time known as the time of fall (t_f), or the dark condition. To put it another way, it is the interval of time between a reaction's 90% and 10% maximum values [14]. Nb_2O_5 thin films were deposited onto a p-type Ge (100) substrate by exposing it to light with a 350 nm wavelength and 104.98 mW/cm^2 intensity.

FOREX Publication
Open Access | Rapid and quality publishing
International Journal of Electrical and Electronics Research (IJEER)
Research Article | Volume 13, Issue 1 | Pages 132-137 | e-ISSN: 2347-470X

While increasing the DC sputtering power from 25W to 50W, we noticed that the surface roughness enhances UV-A photosensitivity to reach maximum value 514.89%. However, as the DC sputtering power was increased to 75 W, the surface roughness also increased, but the photosensitivity decreased to become 371.11%. This decrease may be attributed to detrimental effects associated with further roughening, such as increased surface recombination or reduced film uniformity [13].

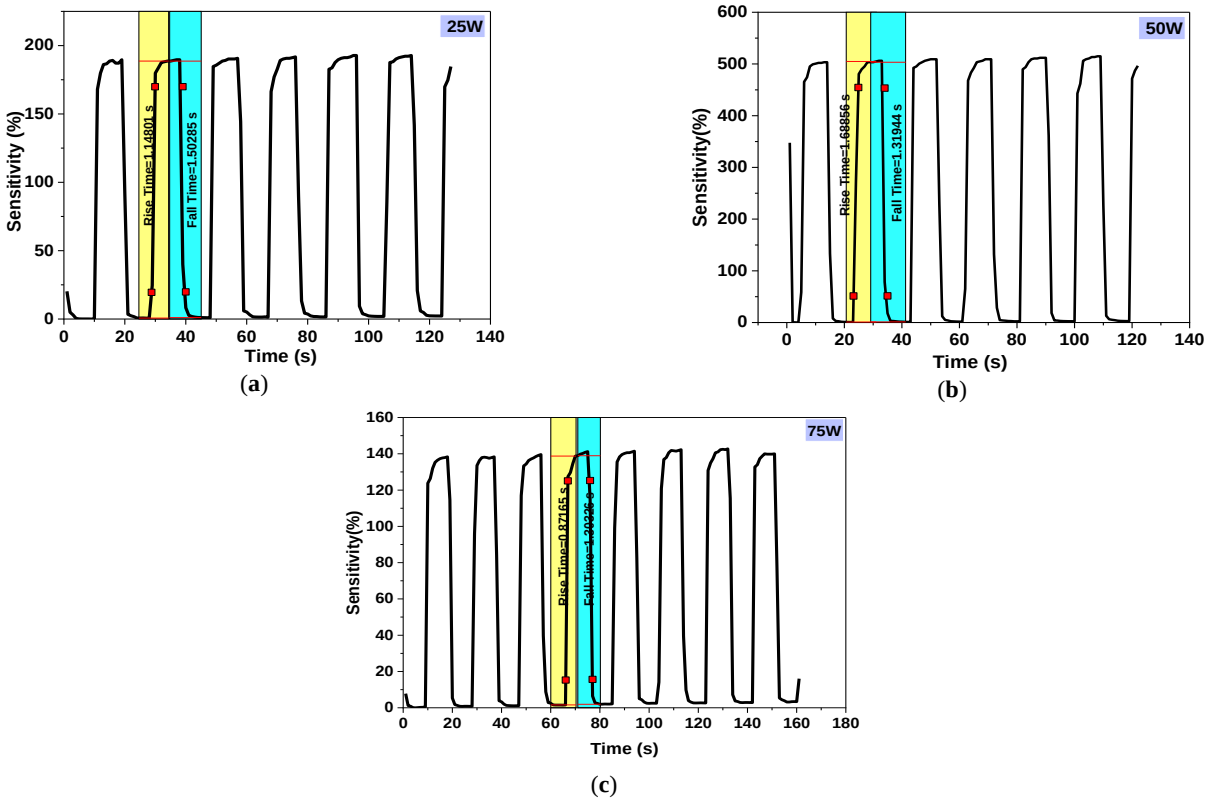

Figure 5. The time-dependent photosensitivity of the Nb_2O_5 thin films made at various powers on/off λ_ex. 350 nm (a) at 25W; (b) at 50W; (c) at 75W

3.5. Cross-section FE-SEM

The determination of Nb_2O_5 thin film thickness deposited on quartz substrates using varied sputtering powers of 25, 50, and 75 W involved tomographic analysis utilizing FESEM, as depicted in *figure 6*. The consistent increase in thickness, ranging from 291 nm to 873 nm, corresponds to the progressive elevation in sputtering power from 25 W to 75 W.

The increase in thin film thickness and sputtering yield with increasing DC sputtering power can be explained by the intensified energy imparted to the sputtering species, typically ions, during higher power deposition. This heightened power induces a more energetic bombardment of the target material, resulting in an increased number of ejected sputtered particles (sputtering yield). Consequently, the accumulation of these particles contributes to an elevation in thin film thickness.

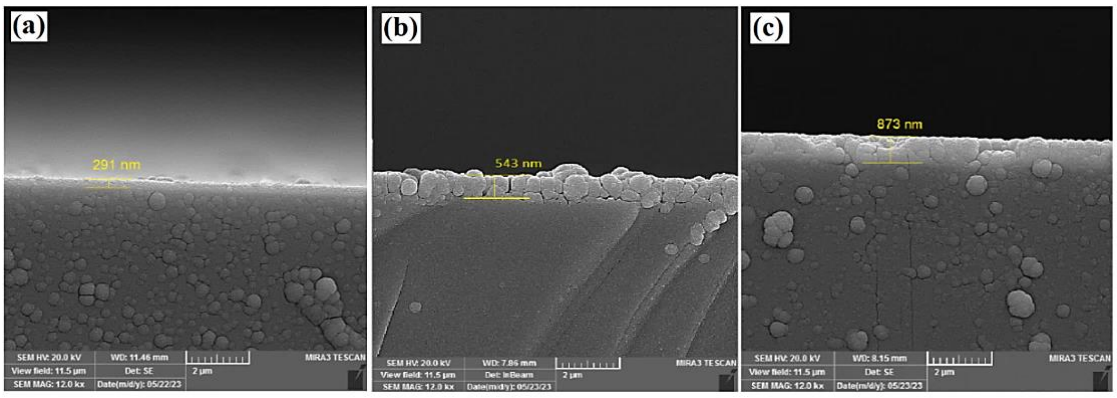

Figure 6. Cross-section FE-SEM images of Nb_2O_5 thin films prepared at different powers (a) 25 W, (b) 50 W, and (c) 75 W

FOREX Publication
Open Access | Rapid and quality publishing
International Journal of Electrical and Electronics Research (IJEER)
Research Article | Volume 13, Issue 1 | Pages 132-137 | e-ISSN: 2347-470X

4. RESULT AND DISCUSSION

This study demonstrated the successful fabrication and characterization of Nb_2O_5 thin films using the DC reactive magnetron sputtering technique, highlighting its potential for producing high-quality metal oxide films. XRD analysis confirmed that the films exhibited a hexagonal polycrystalline crystal structure, with improved crystallinity and larger crystallite sizes observed at higher DC sputtering powers. The uniform deposition of nanostructures, as visualized in FE-SEM images, was significantly influenced by sputtering parameters, emphasizing the critical role of process optimization in determining the films' structural and morphological properties.

A notable finding was the observed decrease in the direct optical energy gap (from 4.46 eV to 3.71 eV) with increasing sputtering power. This trend is attributed to enhanced crystallinity and the reduction of quantum confinement effects, which align with improved film quality and optical performance. UV-Vis spectroscopy revealed strong absorption in the UV region, with optimal performance at 350 nm, indicating the films' applicability for UV-A photodetection.

The most significant result of UV-A photosensitivity was 514.89% at a sputtering power of 50W, demonstrating an optimal balance between surface roughness and uniformity, which enhances light interaction while minimizing detrimental recombination effects. Time-domain response tests confirmed the films' rapid rise and fall times under UV illumination, indicating suitability for real-time and dynamic light-sensing applications.

These findings underscore the potential of Nb_2O_5 thin films for a wide range of applications, including visible-blind UV photodetectors, optoelectronic devices, UV filters, and advanced microelectronics. However, further studies are recommended to explore the films' response across broader wavelengths, varying light-switching frequencies, and different environmental conditions. Such investigations would help refine the understanding of their detection range, dynamic response, and long-term stability, paving the way for enhanced device performance in practical applications.

REFERENCES

[1] Su, K.; Liu, H.; Gao, Z.; Fornasiero, P.; Wang, F. Nb_2O_5-based photocatalysts. *Adv. Sci.* 2021, *8*, 2003156. https://doi.org/10.1002/advs.202003156.

[2] Sayyed, S.A.; Beedri, N.I.; Bhujbal, P.K.; Shaikh, S.F.; Pathan, H.M. Eosin-Y sensitized Bi-layered ZnO nanoflower-CeO2 photoanode for dye-sensitized solar cells application. *ES Mater. Manuf.* 2020, *10*, 45-51. https://doi.org/10.30919/esmm5f939.

[3] Ücker, C.L.; Goetzke, V.; Riemke, F.C.; Vitale, M.L.; de Andrade, L.R.; Ücker, M.D.; Cava, S.S. multi-photonic behavior of Nb_2O_5 and its correlation with synthetic methods. *J. Mater. Sci.* 2021, *56*, 7889-7905. https://doi.org/10.1007/s10853-021-05770-z.

[4] Qi, T.; Wang, Q.; Zhang, Y.; Wang, D.; Yang, R.; Zheng, W. Growth of flower-like SnO2 crystal and performance as photoanode in dye-sensitized solar cells. *Mater. Des.* 2016, *112*, 436-441. https://doi.org/10.1016/j.matdes.2016.09.098.

[5] Akila, Y.; Muthukumarasamy, N.; Agilan, S.; Senthilarasu, S.; Velauthapillai, D. Zirconium oxide post treated tin doped TiO2 for dye sensitized solar cells. *Mater. Sci. Semicond. Process.* 2017, *57*, 24-31. https://doi.org/10.1016/j.mssp.2016.09.028.

[6] Zhang, C.; Chen, S.; Mo, L.E.; Huang, Y.; Tian, H.; Hu, L.; ... & Pan, X. Charge recombination and band-edge shift in the dye-sensitized Mg2+-doped TiO2 solar cells. *J. Phys. Chem. C* 2011, *115*, 16418-16424. https://doi.org/10.1021/jp2024318.

[7] Mehraz, S.; Kongsong, P.; Taleb, A.; Dokhane, N.; & Sikong, L. Large scale and facile synthesis of Sn doped TiO2 aggregates using hydrothermal synthesis. *Sol. Energy Mater. Sol. Cells* 2019, *189*, 254-262. https://doi.org/10.1016/j.solmat.2017.06.048.

[8] Liu, X.; Kong, W.; Zhao, G.; Xuan, J.; Zhao, Y.; Zhou, T.; ... & Yin, G. Enhanced CdS quantum dots loading density and charge transport by Sn4+ doping improve the photoelectrochemical performance of TiO2 nanosheets with highly exposed {001} facets. *Appl. Surf. Sci.* 2019, *486*, 28-36. https://doi.org/10.1016/j.apsusc.2019.04.056.

[9] Mahapatra, A.; Ajimsha, R.S.; Misra, P. Self-powered high responsivity ultraviolet radiation sensor by coupling ZnO based piezoelectric nanogenerator and photodetector. *Appl. Phys. Lett.* 2024, *124*. https://doi.org/10.1063/5.0191001.

[10] Fu, R.; Jiang, X.; Wang, Y.; Li, B.; Ma, J.; Xu, H.; ... & Liu, Y. A high responsivity UV-visible dual band photodetector based on SnO2 microwires with RhB surface sensitization. *J. Alloys Compd.* 2024, *978*, 173533. https://doi.org/10.1016/j.jallcom.2024.173533.

[11] Wang, Y.; Yang, L.; Huang, M.; Kang, Y.; Wang, L.; Zhang, N. A novel self-powered and high switching ratio UV–vis photodetector based on multilayer Bi2O3/In2O3 heterojunction. p*hys. status solidi (RRL)* 2024, *18*, 2300456. https://doi.org/10.1002/pssr.202300456.

[12] Xu, X.; Lu, C.; Wang, Y.; Bai, X.; Liu, Z.; Zhang, Y.; Hua, D. Two dimensional $NbSe2/Nb_2O_5$ metal–semiconductor heterostructure-based photoelectrochemical photodetector with fast response and high flexibility. *Nanoscale Horiz.* 2023, *8*, 1113-1121. https://doi.org/10.1039/d3nh00172e.

[13] Ning, J. ZnTe-Based Photodetectors for Visible-UV Spectral Region. In *Handbook of II-VI Semiconductor-Based Sensors and Radiation Detectors: Volume 2, Photodetectors* 2023, *2*, 281-300. https://doi.org/10.1007/978-3-031-20510-1_12.

[14] Morgenbesser, M.; Schmid, A.; Viernstein, A.; de Dios Sirvent, J.; Chiabrera, F.; Bodenmüller, N.; Fleig, J. SrTiO3 based high temperature solid oxide solar cells: Photovoltages, photocurrents and mechanistic insight. *Solid State Ionics* 2021, *368*, 115700. https://doi.org/10.1016/j.ssi.2021.115700.